ELSEVIER

18 March 1994

Chemical Physics Letters 219 (1994) 331–338

CHEMICAL PHYSICS LETTERS

Duffing's oscillator and the normal to local mode transition in AB_2 triatomic molecules

G.M. Schmid, S. Coy, R.W. Field, R.J. Silbey

Department of Chemistry, Massachusetts Institute of Technology, 77 Massachusetts Avenue, Cambridge, MA 02139, USA

Received 3 December 1993; in final form 18 January 1994

Abstract

We report the analytical solution of the classical equations of motion of Darling–Dennison systems. The solution follows from the equivalence of the system to an undriven Duffing oscillator without damping. The stability properties of the solutions are discussed using phase-plane and potential analysis, resulting in a precise specification of the conditions for the normal to local mode transition. A phase diagram that establishes the correspondence between the classical trajectories to experimentally observed states is presented. The relevance of this result to the quantum mechanical problem is outlined, and the connection to earlier work discussed.

1. Introduction

Localization of vibrational excitation into specific chemical bonds in a molecule is known to affect the rates of chemical reactions. There are two generic mechanisms. First, localization can occur in the presence of a *static* potential induced by some external mechanism. Molecules with broken symmetry in their ground state may exhibit local minima in the associated potential energy surface. Then vibrational excitation is localized in one of these minima at sufficiently low energy. Second, localization can occur in minima of a *dynamic* potential that forms upon excitation of two or more interacting modes, even in the absence of relaxation of excitation. Dynamic symmetry breaking can occur even when the static potential shows no local minima. This is the case for symmetric molecules where it causes the reduction of molecular symmetry.

The object of our study is the class of triatomic molecules of the type AB_2 with C_{2v} symmetry [1,2]. There are two common representations for the Hamiltonian. The normal mode representation is due to Bonner [3] and has been corrected by Darling and Dennison [4], who recognized that the near degeneracy of the symmetric and antisymmetric normal modes requires that the coupling between these two modes be taken into account. The local mode representation is due to Henry and Siebrand [5]. Within an overtone polyad the normal mode representation best predicts the term values for the high-energy states, while the local mode representation is better for the low-energy states. Naturally the question of the physical significance of the different representations arose; for a comprehensive review the reader is referred to ref. [1]. Our work is most closely related to the hindered rotor model by Sibert et al. [6,7] and the local or normal character model by Child and Lawton [8]. Our study is based on the equivalence of the normal mode and local mode representations demonstrated by Lehmann [9] and Kellman [10]. A normal/local classification scheme for the spectral states in terms of the classical trajectories of the Dar-

0009-2614/94/$07.00
SSDI 0009-2614(94)00115-7

ling–Dennison Hamiltonian has been proposed by Xiao and Kellman [11].

Our paper is organized as follows. We give the analytic solution for the classical equations of motion of the Darling–Dennison Hamiltonian. In order to detect dynamical symmetry breaking, we solve for the normalized difference in occupation numbers, i.e. for the probability difference of vibrational excitation of the two local oscillators. Beginning with the local representation of the Darling–Dennison Hamiltonian, we carry out two canonical transformations and then take the classical limit. The probability difference then obeys the equation of motion of an undriven Duffing oscillator without damping. Stationary solutions and stability properties are obtained by standard phase plane analysis. Nonstationary solutions are given in terms of Jacobian elliptic functions. We discuss the dynamics on the basis of the properties of the potential associated with the Duffing oscillator. Furthermore, we will present a phase diagram that establishes 1:1 correspondence between spectral states to the analytic solutions. The conclusion outlines the relevance of this classical analysis to the quantum mechanical Darling–Dennison problem, with emphasis on semiclassical aspects.

2. Analytic solution of the classical equations of motion for Darling–Dennison systems

The quantum mechanical Darling–Dennison Hamiltonian for two coupled stretch vibrations in its local form can be written to good approximation as [10]

$$\hat{H}_{\mathrm{DD}}=\hat{H}_0+\hat{V}_{1:1}\,,$$

$$\hat{H}_0=\omega(\hat{n}+1)+\tfrac{1}{2}\alpha[(\hat{n}_1+\tfrac{1}{2})^2+(\hat{n}_2+\tfrac{1}{2})^2]$$
$$+\alpha_{12}(\hat{n}_1+\tfrac{1}{2})(\hat{n}_2+\tfrac{1}{2})\,,$$

$$\hat{V}_{1:1}=\tfrac{1}{2}[\beta+\tfrac{1}{2}\epsilon(\hat{n}+1)](\hat{a}_1^{\dagger}\hat{a}_2+\hat{a}_2^{\dagger}\hat{a}_1)\,. \tag{1}$$

Here $\hat{a}_i^{\dagger}$ and $\hat{a}_i$, $i=1, 2$, are raising and lowering operators defined by their action on the state of the ith *local anharmonic oscillator*,

$$\hat{a}_i|n_i\rangle=\sqrt{n_i}\,|n_i-1\rangle\,, \tag{2}$$

$$\hat{a}_i^{\dagger}|n_i\rangle=\sqrt{n_i+1}\,|n_i+1\rangle\,. \tag{3}$$

The number operator $\hat{n}_i$ and total number operator $\hat{n}$ are given by

$$\hat{n}_i=\hat{a}_i^{\dagger}\hat{a}_i\,,\quad \hat{n}=\hat{n}_1+\hat{n}_2\,. \tag{4}$$

The Hamiltonian parameters ω, α, α_{12}, β and ϵ are obtained by a non-linear least-squares fit to the spectrum and can be interpreted in terms of the physical picture of two harmonically coupled identical Morse oscillators as follows. ω is the fundamental frequency of the oscillators, α the anharmonicity constant and α_{12} the cross anharmonicity constant. The harmonic coupling $\hat{V}_{1:1}$ increases linearly with the total number of vibrational quanta. A canonical transformation [10] leads to

$$\hat{H}_{\mathrm{DD}}=(\omega+\xi\hat{I})\hat{I}+\hat{C}\,, \tag{5}$$

$$\hat{C}=\zeta\hat{I}_x+\chi\hat{I}_z^2\,, \tag{6}$$

where

$$\hat{I}_x=\hat{a}_1^{\dagger}\hat{a}_2+\hat{a}_2^{\dagger}\hat{a}_1\,, \tag{7}$$

$$\hat{I}_y=-\mathrm{i}(\hat{a}_1^{\dagger}\hat{a}_2-\hat{a}_2^{\dagger}\hat{a}_1)\,, \tag{8}$$

$$\hat{I}_z=\hat{n}_1-\hat{n}_2\,, \tag{9}$$

$$\hat{I}=\hat{n}+1\,, \tag{10}$$

$$\zeta=\tfrac{1}{2}[\beta+\tfrac{1}{2}\epsilon(\hat{n}+1)]\,, \tag{11}$$

and

$$\xi=\tfrac{1}{4}(\alpha+\alpha_{12})\,, \tag{12}$$

$$\chi=\tfrac{1}{4}(\alpha-\alpha_{12})\,. \tag{13}$$

Note that since $\hat{I}$ and $\hat{H}_{\mathrm{DD}}$ are constants of motion so then is $\hat{C}$. In particular $\langle\hat{I}(t)_z\rangle/\langle\hat{I}\rangle=\mathscr{I}_z$ can be interpreted as the normalized difference in occupation numbers of the equivalent local oscillators, and is diagnostic of localization. In order to solve for this quantity in the classical limit we carry out a new canonical transformation such that $\hat{I}_z$, $\dot{\hat{I}}_z$ are conjugate variables to find

$$\hat{H}=2[\zeta^2(\hat{I}^2-\hat{1})-\hat{C}^2]$$
$$=2(\zeta\hat{I}_y)^2-2\chi\{\hat{C},\hat{I}_z^2\}+2\zeta^2\hat{I}_z^2+2\chi^2\hat{I}_z^4\,, \tag{14}$$

$$\{\hat{C},\hat{I}_z^2\}=\hat{C}\hat{I}_z^2+\hat{I}_z^2\hat{C}\,. \tag{15}$$

By construction we have

$$[\hat{H}_{\mathrm{DD}},\hat{H}]=0\,. \tag{16}$$

For highly excited states the classical limit provides a

good approximation. The operators $\frac{1}{2}\hat{I}$, $\frac{1}{2}\hat{I}_x$, $\frac{1}{2}\hat{I}_y$, $\frac{1}{2}\hat{I}_z$ then correspond to the actions $\frac{1}{2}I$, $\frac{1}{2}I_x$, $\frac{1}{2}I_y$, $\frac{1}{2}I_z$, $\hat{a}_i$ to the complex amplitudes a_i, and $\hat{\zeta}$, $\hat{C}$ to the numbers ζ, C. H_{DD} and H take the form

$$H_{DD}=(\omega+\xi I)I+C\,, \tag{17}$$

$$I^2=I_x^2+I_y^2+I_z^2\,, \tag{18}$$

$$C=\zeta I_x+\chi I_z^2\,. \tag{19}$$

$$H=T+V\,, \tag{20}$$

$$T=2(\zeta I_y)^2\,, \tag{21}$$

$$V=\tfrac{1}{2}AI_z^2+\tfrac{1}{4}BI_z^4\,, \tag{22}$$

$$\mathrm{A}=(2\zeta)^2-8\chi C\,, \tag{23}$$

$$B=8\chi^2\,, \tag{24}$$

and share the dynamical invariants I, C. Let us denote the associated energies by E_{DD}, E. Note the dependence of A on initial conditions via C. The equations of motion are now given by the Poisson brackets

$$\dot{I}_z=\{I_z, H_{DD}\}=\{I_z, H\}=\partial_{I_x}H\,, \tag{25}$$

$$\dot{I}_z=\{\dot{I}_z, H_{DD}\}=\{\dot{I}_z, H\}=-\partial_{I_z}H\,. \tag{26}$$

H is identical to the Hamiltonian of an *undriven Duffing oscillator without damping*. The explicit form of Eq. (26),

$$-\delta_{I_z}V(I_z)=\dot{I}_z=-AI_z-BI_z^3\,, \tag{27}$$

is known as the *Duffing equation*. It is easily explicitly verified that I_z obeys the same dynamical equation using H_{DD} as the generating function.

We obtain the *stationary solutions* $S(\mathcal{I}_x, \mathcal{I}_y, \mathcal{I}_z)$ and their stability properties by phase plane analysis in the normalized coordinates

$$\mathcal{I}_{x,y,z}=\frac{I_{x,y,z}}{I}\,. \tag{28}$$

Furthermore we introduce the dimensionless parameter κ,

$$\kappa=\frac{\zeta}{2\chi I}=\frac{\frac{1}{2}\epsilon+\beta/I}{\alpha-\alpha_{12}}\,. \tag{29}$$

For $|\kappa|>1$ we find two center points (neutrally stable), $S^{1,2}=(\pm1, 0, 0)$. For $|\kappa|<1$ we find four stationary points, $S^{1,2}=(\pm1, 0, 0)$, $S^{3,4}=(\kappa, 0, \pm\sqrt{1-\kappa^2})$: for $\kappa>0$, S^1 is a saddle point (unstable), $S^{2,3,4}$ are center points; for $\kappa<0$, $S^{1,3,4}$ are center points, S^2 is a saddle point.

There are two bifurcations: A pitchfork bifurcation at $|\kappa|=1$ and a transcritical bifurcation at $\kappa=0$. This shows, as expected, that the Duffing Hamiltonian has the same stability properties as the Darling–Dennison Hamiltonian discussed by Lie et al. [12]. The bifurcation diagram is shown in Fig. 1.

The *nonstationary solutions* to the Duffing equation are known to be of the form [13]

$$\mathcal{I}_z(t)=Df(\Omega t-\Phi\,|\,m)\,. \tag{30}$$

Here f is a Jacobian elliptic function with amplitude D, frequency Ω, phase Φ and parameter m. There are three types of such functions that are relevant here, denoted by cn, dn and nd. Inserting in Eq. (27) and using Eqs. (18) and (19) one obtains three qualitatively different solutions, depending on the parameter m.

For $m>1$ the solution is given by

$$\mathcal{I}_z=D\,\mathrm{dn}(\sqrt{m}[\Omega t-\Phi_{\mathrm{dn}}]\,|\,1/m)\,, \tag{31}$$

$$\Phi_{\mathrm{dn}}=-\frac{1}{\sqrt{m}}F\left(\arcsin\sqrt{\frac{1-[\mathcal{I}_z(t_0)/D]^2}{m}}\,\middle|\,\frac{1}{m}\right).$$

For $0<m<1$ the solution is given by

$$\mathcal{I}_z=D\,\mathrm{cn}(\Omega t-\Phi_{\mathrm{cn}}\,|\,m)\,, \tag{32}$$

$$\Phi_{\mathrm{cn}}=-F(\arccos[\mathcal{I}_z(t_0)/D]\,|\,m)\,.$$

For $m<0$ the solution is given by

$$\mathcal{I}_z=D\,\mathrm{nd}\left(\sqrt{1+|m|}\;[\Omega t-\Phi_{\mathrm{nd}}]\,|\,\frac{1}{1+|m|}\right), \tag{33}$$

$$\Phi_{\mathrm{nd}}=-\frac{1}{\sqrt{1+|m|}}\times F\left(\arcsin\sqrt{\frac{1-[D/\mathcal{I}_z(t_0)]^2}{m}}\,\middle|\,\frac{1}{1+|m|}\right).$$

The values of D, m, Ω for the Darling–Dennison problem are

$$D=\pm\frac{1}{I}\sqrt{-\frac{A}{B}+2\kappa I\sqrt{I^2(1-\kappa^2)+\frac{A}{B}}}\,, \tag{34}$$

$$m=\frac{1}{2}\left(1-\frac{A/B}{2\kappa I\sqrt{I^2(1-\kappa^2)+A/B}}\right), \tag{35}$$

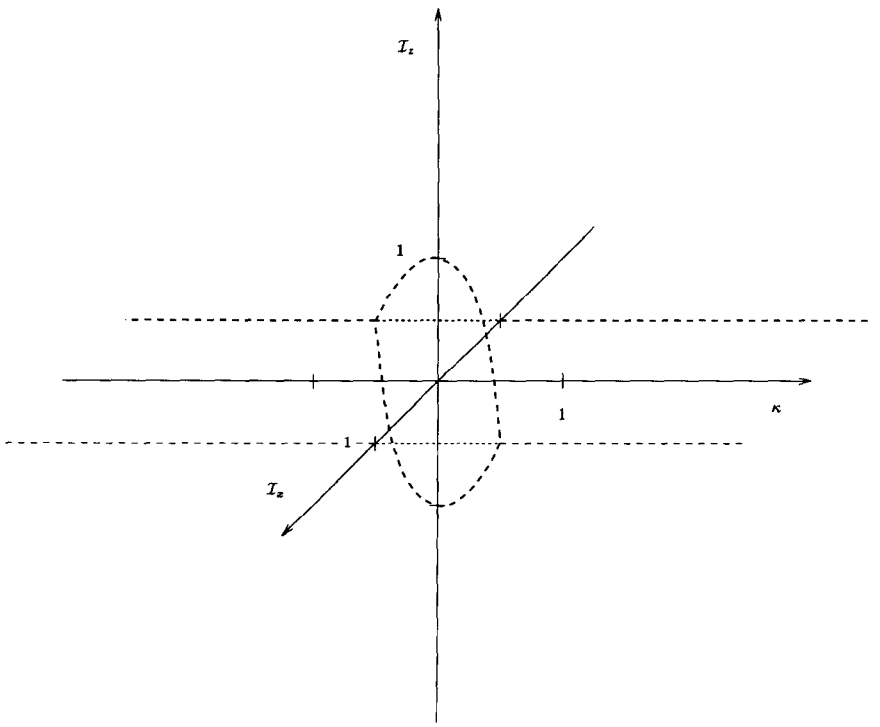

Fig. 1. Bifurcation diagram for Eq. (27) (without damping). Dashed lines indicate neutrally stable branches, dotted lines unstable branches.

$$\Omega = \frac{DI}{2\kappa\sqrt{m}}. \tag{36}$$

Here cn, dn, nd are Jacobian elliptic functions and F is an elliptic integral of the first kind. Fig. 2 shows the elliptic functions for different values of the parameter m. Note that the frequency Ω depends on the initial amplitude D. The trajectories are obtained as follows. The solutions for I_x, I_y follow from the definition of C and I in Eqs. (18) and (19). Consequently, from the definitions of I_x, I_y, I_z we can obtain the solution for the complex amplitudes a_i. Finally, the knowledge of a_i enables us to solve for the trajectories [2].

3. Discussion

Let us begin with a discussion of the solutions for $\mathcal{I}_z$.

The cn function oscillates between the upper bound D and lower bound $-D$. Thus the vibrational excitation is completely transferred from one oscillator to the other after two quarterperiods, which are usually denoted by $K=F(\pi/4\,|\,m)$. The associated level has normal character.

The dn function oscillates with an upper bound D (or lower bound $-D$) but does not change sign. Thus the vibrational excitation is never completely transferred. The associated level has local character.

The nd function oscillates with a lower bound D (or upper bound $-D$) and thus describes motion in the localized regime as well. Whereas under dn evolution the excitation appears to be attracted by the initially less excited local oscillator, under nd evolution it appears to be repelled. A close examination of the phase plane reveals that this distinction is superficial.

Let us check the two limiting regimes of vanishing anharmonicity and of vanishing coupling for the case of an initially local excitation for large $I \approx n$, i.e. $\mathcal{I}_z(t_0)=1$. From Eqs. (34)–(36) we obtain $D=1$, $m=1/4\kappa^2$, $\Omega=2\zeta$. In the limit of vanishing anharmonicity $\chi\to 0$, $\kappa\to\infty$, the vibrational excitation oscillates freely between the local oscillators, since

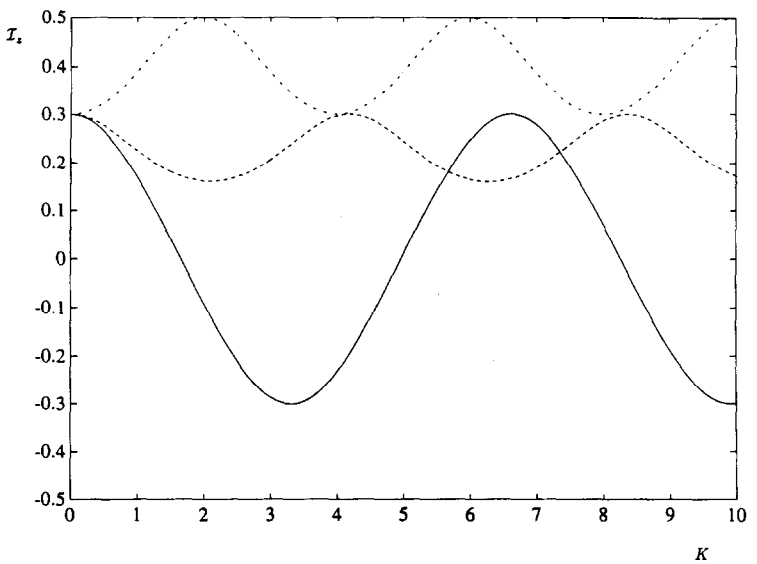

Fig. 2. Jacobian elliptic functions cn, dn, nd. The abscissa is given in units of $K=F(\pi/4|m=1.4)$, $D=0.3$, $\Phi=0$. The solid line indicates $\mathrm{cn}(Kt|0.2)$, the dashed line $\mathrm{dn}(Kt|m=0.7)$ and the dash-dotted line $\mathrm{nd}(Kt|0.7)$.

$m\to 0$, and $\mathcal{I}_z=\mathrm{cn}(2\zeta t|m)\to\cos(2\zeta t)$. In the limit of no coupling $\zeta\to 0$, $\kappa\to 0$, the initial distribution of vibrational excitation is maintained at all times, since $m\to\infty$, and $\mathcal{I}_z=\mathrm{dn}(2\zeta t|1/m)\to 1$.

The transitions between the different dynamic regimes depend on the parameter m, which is connected to the bifurcation parameter κ and the potential V.

The bifurcation parameter κ relates not only the antagonistic tendencies of transfer and localization of vibrational excitation but also takes the total excitation into account. The transfer tendency is represented by the coupling parameter ζ. ζ increases linearly with I. Large values of ζ favor transfer. The localization tendency is represented by the parameter χ. χ is given by the local anharmonicity constant reduced by the cross anharmonicity constant. Large values of χ favor localization. The division by I appears upon transforming the Duffing equation into dimensionless normalized coordinates. There are three things to notice: (1) $|\kappa|$ takes different values for different molecular species. It characterizes the overall tendency towards local or normal behavior. Small values of $|\kappa|$ indicate local behavior, large values normal behavior. (2) $|\kappa|$ decreases with increasing I. (3) Only the magnitude of κ is relevant for the dynamical properties. Two completely different physical situations such as a sign change of the Hamiltonian parameters can lead to identical properties regarding the transfer of vibrational excitation.

The potential $V(I_z)$ is *static* in I_z, yet due to its dependence on the momenta of the local oscillators, *dynamic* in the original coordinates. For nonnegative A it is a single well potential, otherwise a double well potential. The sign change in the potential parameter A and thus the transition from a single well to a double well potential occurs at $m=\frac{1}{2}$ under the necessary condition $|\kappa|<1$. The depth of the well and thus the height of the potential barrier can be calculated to be

$$E=-\chi^2(1-\kappa^2)I^4\,. \tag{37}$$

The sign change in the total energy E of the Duffing oscillator and thus the drop of the kinetic energy below the top of the potential energy barrier between the wells occurs at $m=1$. For a given set of Hamiltonian parameters, the signs of both A and E depend on the initial conditions via the dynamical invariant C.

The dependence on initial conditions is best displayed in a phase diagram spanned by $\mathcal{I}_z(t_0)$ and $\mathcal{I}_x(t_0)$. The inequality $\mathcal{I}_z^2(t_0)+\mathcal{I}_x^2(t_0)\leqslant 1$ restricts the accessible area of the phase diagram to the unit circle. The three different dynamic regimes are separated by two curves.

The regions of single and double well potentials are separated by the *bifurcation parabola*

$$\mathcal{J}_x^{\mathrm{b}}(t_0)=\kappa-\frac{\mathcal{J}_z^2(t_0)}{2\kappa}. \tag{38}$$

The regions for which $E>0$ and $E<0$ are separated by the *localization parabola*

$$\mathcal{J}_x^{\mathrm{s}}(t_0)=\pm 1-\frac{\mathcal{J}_z^2(t_0)}{2\kappa}. \tag{39}$$

For $\kappa>0$ the ordinate must be taken positive, for $\kappa<0$ negative.

A state observed in the spectrum at energy E_{DD} appears in the phase diagram as the *spectral parabola*

$$\mathcal{J}_x^{\lambda}(t_0)=\mathscr{E}-\frac{\mathcal{J}_z^2(t_0)}{2\kappa}, \tag{40}$$

$$\mathscr{E}=\frac{1}{\zeta I}\left[E_{\mathrm{DD}}-(\omega+\xi I)I\right], \quad \mathscr{E}=\frac{C}{I}. \tag{41}$$

The stationary points lie on the unit circle and have for $|\kappa|<1$ the coordinates $(\pm\sqrt{1-\kappa^2},\kappa)$.

Fig. 3 displays the spectral states in the phase diagram for H_2O, $I=6$ and SO_2, $I=6$. Without loss of generality let us restrict ourselves to the discussion of $\kappa>0$. The area of the phase diagram within the unit circle is divided into three regions by the two parabolae, $\mathcal{J}_x^{\mathrm{s}}(t_0)$, $\mathcal{J}_x^{\mathrm{b}}(t_0)$, indicated as solid lines. For $\mathscr{E}>1$ the corresponding $\mathcal{J}_x^{\lambda}(t_0)$, indicated as a dashed line, lies in the region of modes of local character. For $1>\mathscr{E}>\kappa$ the corresponding $\mathcal{J}_x^{\lambda}(t_0)$ lies in the region of modes of normal character in a double well potential. For $\kappa>\mathscr{E}$ the corresponding $\mathcal{J}_x^{\lambda}(t_0)$ lies in the region of modes of normal character in a single well potential. It can be shown that at $\mathscr{E}=\kappa$, $m=0.5$ and at $\mathscr{E}=1$, $m=1$. This establishes the connection between m, κ and V. It can easily be deduced that the necessary condition for the existence of modes of local character is that $|\kappa|<1$.

We briefly mention the relation of our results to other work. The surface that allows the complete representation of the results of the phase plane analysis is given by the Poincaré sphere. In the context of molecular dynamics it is described as the *polyad phase sphere*. The phase diagram can be trivially extended to a phase profile on the sphere by introducing $\mathcal{J}_y$ as the third axis. The trajectories then appear as closed curves on the sphere. Now we can interprete the dynamics in the single or double well potential V as dynamics in the harmonic potential $\mathscr{E}$ under the constraint of motion on a sphere [14]. The trajectories on the phase sphere can be geometrically constructed from the dynamical invariants C, I. The classification of spectral states by the properties of the phase space trajectories is due to Kellman [10,11].

An analysis of the explicit form of the complex am-

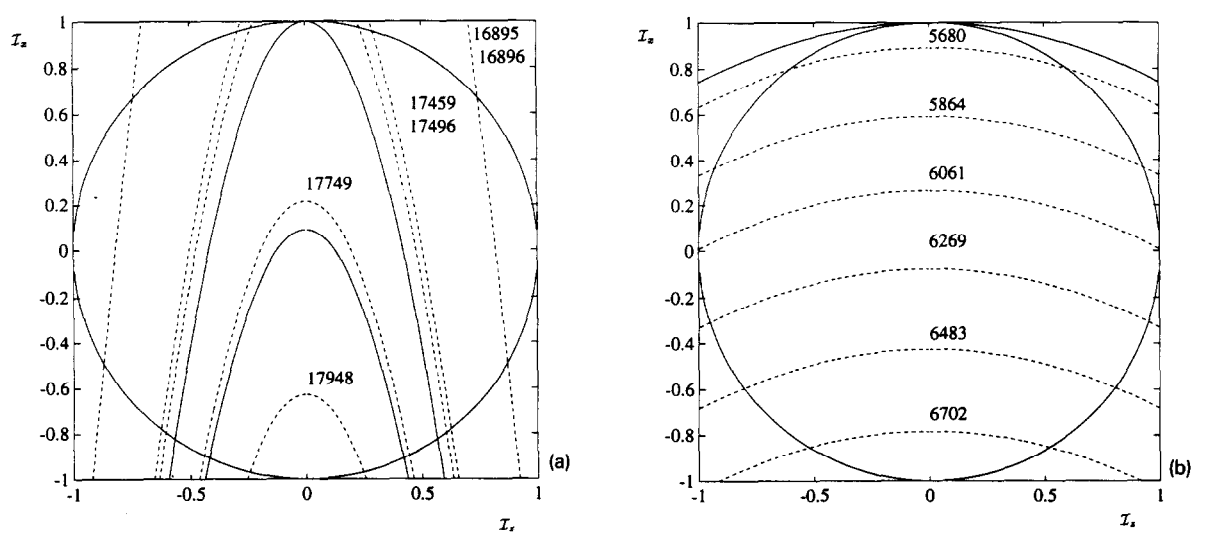

Fig. 3. Phase diagrams for H_2O and SO_2, $I=6$, the Hamiltonian constants are adapted from ref. [10]. The bifurcation parabola and the localization parabola are indicated as solid lines, spectral parabolae as dashed lines. The wavenumber of each transition is given above the corresponding parabola. (a) For H_2O, $\kappa(6)=0.09$, there are four states of local character, (b) for SO_2, $\kappa(6)=1.96$, all states are of normal character.

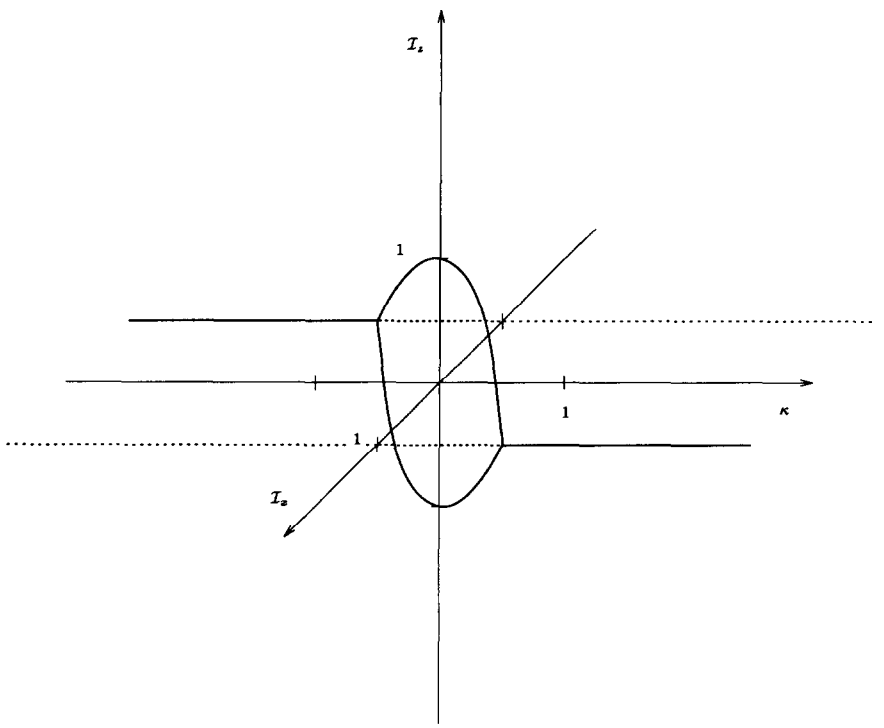

Fig. 4. Bifurcation diagram for the damped system under conservation of I. Solid lines indicate stable branches, dotted lines unstable branches.

plitudes reveals that the difference of the phase angles of the local oscillators can sweep full cycles only if the vibrational excitation *cannot* be completely exchanged. This result was derived by Sibert et al. [6] using the hindered rotor model, based on earlier work by Jaffe and Brumer [15]. The solutions for the dynamics of the energy transfer are as well solutions to the Duffing oscillator. Thus the rates of energy transfer obtained from trajectory calculations have to match this result.

The similarity of the parameter κ to the local mode parameter used by Child and Lawton [8] is striking. It differs in that κ takes the amount of vibrational excitation into account.

Finally, it is worth mentioning, that preceding transformations can be carried out for a variety of different couplings $V_{k:l}$. In particular $V_{2:2}$ leads to a Duffing equation as well. Furthermore the generalization to damped systems under conservation of I is straightforward and relevant for the dynamics in condensed systems. The number and location of stationary points is the same as for the undamped case, yet the stability properties are different. The bifurcation diagram is shown in Fig. 4.

4. Conclusion

The mapping of the Darling–Dennison Hamiltonian onto the Duffing Hamiltonian goes far beyond the obvious benefit of obtaining an analytic solution for the classical trajectories. In particular, the potential V allows intuitive insight into the classical properties of the system and qualitative predictions of quantum mechanical properties. This potential V is new having been derived from a canonical transformation in contrast to the potentials studied by previous workers [6,10].

The exchange of vibrational excitation behaves in the classical limit like a particle in a single or double well potential. The important difference from the standard Duffing oscillator is that the potential parameter A depends on the initial conditions. In particular, the potential barrier forms and grows upon

excitation. As opposed to the standard Duffing oscillator, the modes of local character become unstable *upon* excitation and *not* on relaxation of the system. The parameter κ describes the *global* tendency of a certain molecular species to form modes of local or normal character. The question of the local or normal character of each *individual* state with energy E_{DD} can be decided by comparing the magnitude of the normalized invariant $\mathscr{C}$ to κ, regardless of the underlying physical phenomenon.

Furthermore the potential V provides an intuitive explanation for two observations in the quantum mechanical Darling–Dennison Hamiltonian: that the number of states of local character and that their locality increases with I. Using semiclassical ideas one can make the following predictions. For the case of a single well the spectrum consists of almost equidistant states of normal character. Upon excitation the potential barrier forms and grows. The spectrum splits in two regions. For energies above the barrier it contains almost equidistant states of normal character, while for energies below the barrier, there are almost-degenerate pairs of states of local character. Since the potential barrier grows like I^4, the limit of near degeneracy and thus high locality is attained for relatively small I. The time required for an initially localized state to pass over or to tunnel through the barrier is then approximated by the inverse splitting. Let us compare the timescales involved for the complete transfer of an initially localized wavepacket with energy below the barrier, and thus large components along the local character eigenstates, to an initially localized wavepacket with energy above the barrier, and thus large components along the normal character eigenstates. The wavepacket with energy below the barrier remains local during a period of transfer of the wavepacket above the barrier. Thus the distinction between of states of local or normal character can be justified from the point of view of *dynamics*.

The present treatment covers only the dynamics in the local or normal regimes. The process of localization can be classically modelled by the introduction of damping in the presence of small perturbations and has been briefly indicated above. In a forthcoming paper [16], we will report new results on the quantum mechanical treatment of the Darling–Dennison Hamiltonian that establish the full connection to the classical treatment presented here. We will give a physical interpretation of the notions of local character, normal character and localization. That interpretation is supported by a quantitative measure of the susceptibility of quantum states to symmetry breaking perturbations.

References

[1] M.S. Child and L. Halonen, Advan. Chem. Phys. 57 (1984) 1.
[2] C.C. Rankin and W.H. Miller, J. Chem. Phys. 35 (1971) 3150.
[3] L.G. Bonner, Phys. Rev. 46 (1934) 458.
[4] B.T. Darling and D.M. Dennison, Phys. Rev. 57 (1940) 128.
[5] B.R. Henry and W. Siebrand, J. Chem. Phys. 49 (1968) 5369.
[6] E.L. Sibert III, W.P. Reinhardt and J.T. Hynes, J. Chem. Phys. 77 (1982) 3583.
[7] E.L. Sibert III, W.P. Reinhardt and J.T. Hynes, J. Chem. Phys. 77 (1982) 3595.
[8] M.S. Child and R.T. Lawton, Faraday Discussions Chem. Soc. 71 (1981) 273.
[9] K.K. Lehmann, J. Chem. Phys. 79 (1983) 1098.
[10] M. Kellman, J. Chem. Phys. 83 (1985) 3842.
[11] L. Xiao and M. Kellman, J. Chem. Phys. 90 (1989) 6086.
[12] Z. Li, L. Xiao and M. Kellman, J. Chem. Phys. 92 (1990) 2251.
[13] D.F. Lawden, Elliptic functions and applications (Springer, Berlin, 1989).
[14] V.I. Arnold, Mathematical methods of classical mechanics, 2nd Ed. (Springer, Berlin, 1989) p. 469ff.
[15] C. Jaffe and P. Brumer, J. Chem. Phys. 73 (1980) 5646.
[16] G.M. Schmid, S. Coy, R.W. Field and R.J. Silbey, to be published.